
Complete the Missing Half: Augmenting Aggregation Filtering with Diversification for Graph Convolutional Networks

Sitao Luan^{1,2,*}, Mingde Zhao^{1,2,*}, Chenqing Hua^{1,*}, Xiao-Wen Chang¹, Doina Precup^{1,2,3}
 {sitao.luan@mail, mingde.zhao@mail, chenqing.hua@mail, chang@cs, dprecup@cs}.mcgill.ca

¹McGill University; ²Mila; ³DeepMind

*Equal Contribution

Abstract

The core operation of Graph Neural Networks (GNNs) is the *aggregation* enabled by the graph Laplacian or message passing, which filters the neighborhood information of the nodes. Though effective for various tasks, they are the potentially problematic factor of all GNN methods, as they force the node representations to be similar, making the nodes gradually lose their identity and become indistinguishable. In this paper, we augment the aggregation operations with their dual, *i.e.* diversification operators that make the node more distinct and preserve the identity. Such augmentation replaces the aggregation with a two-pass filtering process that, in theory, is beneficial for enriching the node representations. In practice, the two-pass filters can be easily patched on existing GNN methods with diverse training strategies, including spectral and spatial (message passing) methods. When patched on baselines, we observe the significant performance boost on 8 node and graph classification tasks.

1 Introduction

As a generic data structure, graph is capable of modeling complex relationships among objects in many real-world problems [20, 23, 7]. Analogous to the convolution operator defined on images in Convolutional Neural Networks (CNNs) [19], spectral- and spatial-based graph convolutions [30] are defined on the graph Fourier domain and the node spatial neighborhood domain [34]. Based on the 2 methodologies, different (linear) graph filters and (non-linear) deep learning techniques [18] are combined, giving rise to Graph Neural Networks (GNNs), which have achieved remarkable progress [2, 14, 11, 17, 27, 21].

Essentially vertex localization, graph filters can be viewed as operators that aggregate node information from the direct neighbors. Different graph filters yield different spectral GNNs and spatial aggregation functions. Among them, the most commonly used is the *renormalized Laplacian*, proposed in [17]. By adding an identity matrix to the adjacency matrix, *i.e.* a self-loop in graph topology, renormalized graph Laplacian is essentially a low-pass filter [22] capturing low-frequency signals, *i.e.* locally smooth features, across the whole graph [29]. Aggregation processes, in the form of message passing used in spatial-based methods, *e.g.*, GraphSAGE [14] and GAT [27], are also node-level Low-Pass (LP) filters which make each node become more similar to the neighbors. Both LP filter and node aggregation are devised upon the following assumptions.

Assumption 1 Low-frequency components of the input features are sufficient to predict the output: connected nodes share similar representations as the output is a smooth function over the graph.

Assumption 2 The high-frequency components are noises and should be filtered out or attenuated, because they provide nothing but harmful information for representation learning.

In the methods built upon those conceptions, the distinctiveness of each node or individual is gradually wiped out and we merely focus on the global property of the whole community. It is natural to realize that these assumptions may not hold for outliers and boundary nodes, as they are highly likely to be different than the insiders. Also, the aggregation operations inevitably cause the loss of information distinctive to the nodes, potentially causing the inability to learn better representations.

With these in mind, in this paper, we argue that to learn more robust representations, the distinctive information of nodes should also be extracted with an operator, resembling extraction of the mutual information enabled by the aggregation operator. To enable such bipolar learning, we utilize both LP and High-Pass (HP) filters, one for aggregation and another for diversification. We will present analyses backing our belief, which consider operations from the perspective of graph signal filters, and discuss in details how to deal with the augmented graph filtering appropriately.

The rest of the paper is organized as follows. In Section 2, we introduce the backgrounds for graph convolution, graph filters and filterbanks; In Section 3, we illustrate the motivation of adding HP filter in GNN and introduce three indivisible components which are necessary for enabling 2-pass filter learning; In section 4, we propose FB-GNN (Filter Bank GNN) by assembling the three components, which can be easily patched on spectral- and spatial-based methods; Finally, in Section 5, we validate the empirical effectiveness of our ideas on several node classification tasks and graph classification tasks.

2 Preliminaries

We use bold fonts for vectors (*e.g.*, v), block vectors (*e.g.*, V) and matrix blocks (*e.g.*, V_i). Suppose we have an undirected connected graph $\mathcal{G} = (\mathcal{V}, \mathcal{E}, A)$ without bipartite component, where \mathcal{V} is the node set with $|\mathcal{V}| = N$, \mathcal{E} is the edge set with size $|\mathcal{E}| = E$, $A \in \mathbb{R}^{N \times N}$ is a symmetric adjacency matrix with $A_{ij} = 1$ if and only if $e_{ij} \in \mathcal{E}$ otherwise $A_{ij} = 0$, D is the diagonal degree matrix, *i.e.* $D_{ii} = \sum_j A_{ij}$ and $\mathcal{N}_i = \{j : e_{ij} \in \mathcal{E}\}$ is the neighborhood set of node i . A graph signal is a vector $\mathbf{x} \in \mathbb{R}^N$ defined on \mathcal{V} , where x_i is defined on the node i . We also have a feature matrix $\mathbf{X} \in \mathbb{R}^{N \times F}$ whose columns are graph signals and each node i has a feature vector $\mathbf{X}_{i,:}$ with dimension F , which is the i -th row of \mathbf{X} .

Graph Laplacian and Affinity Matrix The (Combinatorial) graph Laplacian is defined as $L = D - A$, which is a Symmetric Positive Semi-Definite (SPSD) matrix[4]. Its eigendecomposition gives $L = U\Lambda U^T$, where the columns of $U \in \mathbb{R}^{N \times N}$ are orthonormal eigenvectors, namely the *graph Fourier basis*, $\Lambda = \text{diag}(\lambda_1, \dots, \lambda_N)$ with $\lambda_1 \leq \dots \leq \lambda_N$ and these eigenvalues are also called *frequencies*. The graph Fourier transform of the graph signal \mathbf{x} is defined as $\mathbf{x}_F = U^{-1}\mathbf{x} = U^T\mathbf{x} = [\mathbf{u}_1^T\mathbf{x}, \dots, \mathbf{u}_N^T\mathbf{x}]^T$, where $\mathbf{u}_i^T\mathbf{x}$ is the component of \mathbf{x} in the direction of \mathbf{u}_i . Some variants of graph Laplacians are commonly used in practice, *e.g.*, the symmetric normalized Laplacian $L_{\text{sym}} = D^{-1/2}LD^{-1/2} = I - D^{-1/2}AD^{-1/2}$, the random walk normalized Laplacian $L_{\text{rw}} = D^{-1}L = I - D^{-1}A$. L_{rw} and L_{sym} share the same eigenvalues, which are inside $[0, 2]$, and their corresponding eigenvectors satisfy $\mathbf{u}_{\text{rw}}^i = D^{-1/2}\mathbf{u}_{\text{sym}}^i$.

The affinity (transition) matrix derived from L_{rw} is defined as $P_{\text{rw}} = I - L_{\text{rw}} = D^{-1}A$ and its eigenvalues $\lambda_i(P_{\text{rw}}) = 1 - \lambda_i(L_{\text{rw}}) \in (-1, 1]$. Similarly, $P_{\text{sym}} = I - L_{\text{sym}} = D^{-1/2}AD^{-1/2}$ is an affinity matrix as well. Renormalized affinity matrix is introduced in [17] and defined as $\hat{A}_{\text{rw}} = \tilde{D}^{-1}\tilde{A}$, where $\tilde{A} \equiv A + I$, $\tilde{D} \equiv D + I$ and $\lambda(\hat{A}_{\text{rw}}) \in (-1, 1]$. It essentially defines a random walk matrix on \mathcal{G} with a self-loop added to each node in \mathcal{V} and is widely used in GCN as

follows,

$$\mathbf{Y} = \text{softmax}(\hat{A}_{\text{rw}} \text{ReLU}(\hat{A}_{\text{rw}} \mathbf{X} W_0) W_1) \quad (1)$$

where $W_0 \in \mathbb{R}^{F \times F_1}$ and $W_1 \in \mathbb{R}^{F_1 \times O}$ are parameter matrices. $\hat{A}_{\text{sym}} \equiv \tilde{D}^{-1/2} \tilde{A} \tilde{D}^{-1/2}$ can also be applied in GCN. Specifically, the nature of transition matrix makes \hat{A}_{rw} behave as a mean aggregator ($\hat{A}_{\text{rw}} \mathbf{x}$) $_i = \sum_{j \in [N_i \cup i]} x_j / (D_{ii} + 1)$ which is applied in [14] and is important to bridge the gap between spatial- and spectral-based graph convolution methods.

Lazy Random Walk The transition matrix Z_{rw} of a lazy random walk on \mathcal{G} can be expressed by P_{rw} easily: $Z_{\text{rw}} = (I + P_{\text{rw}})/2$ [3], *i.e.* at each step, we flip a fair coin to decide if to stay or move according to P_{rw} . This can also be seen as adding D_{ii} self-loops to the i -th node on A and normalize it to a transition matrix and $0 \leq \lambda_i(Z_{\text{rw}}) \leq 1$. We can also have lazy symmetric affinity matrix $Z_{\text{sym}} = (I + D^{-1/2} A D^{-1/2})/2$. We can define generalized lazy random walk by $Z_{\text{rw}}^\gamma = (\gamma I + P_{\text{rw}})/(1 + \gamma)$, where γ is a self-loop parameter. Its symmetric version is $Z_{\text{sym}}^\gamma = (\gamma I + P_{\text{sym}})/(1 + \gamma)$. Unlike \hat{A}_{rw} , Z_{rw} maintains certain topology properties of P_{rw} , *e.g.*, stationary distribution and eigenvectors. Unless one has enough prior knowledge that the reformed matrix works better, they are thought not supposed to be changed.

LP, HP Graph Filters and Filter Banks The smaller eigenvalue λ_i of graph Laplacian L indicates larger global smoothness (low frequency) of \mathbf{u}_i [5]. This means any two elements of \mathbf{u}_i corresponding to two connected nodes will have similar values. The multiplication of L and \mathbf{x} acts as a filtering operation over \mathbf{x} , adjusting the scale of the components of graph signal in frequency domain. To see this, consider

$$\mathbf{x} = \sum_i \mathbf{u}_i \mathbf{u}_i^T \mathbf{x}, \quad L\mathbf{x} = \sum_i \lambda_i \mathbf{u}_i \mathbf{u}_i^T \mathbf{x} \quad (2)$$

The projection $\mathbf{u}_i \mathbf{u}_i^T \mathbf{x}$ corresponding to a large $|\lambda_i|$ will be amplified, while the one corresponding to a small $|\lambda_i|$ will be suppressed. More specifically, a graph filter that filters out smooth (bumpy) components is called HP (LP) filter. Generally, both L_{sym} and L_{rw} can be regarded as HP filters [9]. P_{rw} and P_{sym} can be treated as LP filters, while they actually both remove intermediate frequency components [22].

On the node level, left multiplying L_{rw} or P_{rw} on \mathbf{x} can be understood as diversification and aggregation operations, respectively. For the i -th node,

$$(L_{\text{rw}} \mathbf{x})_i = \sum_{j \in N_i} \frac{1}{D_{ii}} (x_i - x_j), \quad (P_{\text{rw}} \mathbf{x})_i = \sum_{j \in N_i} \frac{1}{D_{ii}} x_j \quad (3)$$

Thus, aggregation and diversification can be seen as node-level LP and HP filters. Intuitively, bumpy projection components depict the differences between a node and its neighbors, making it distinguishable; While smooth projection components focus on the similarity within a neighborhood, from which we can obtain missing or unknown feature of the node. We believe that these two conjugate components are both indispensable to portray a node.

A two-channel linear filterbank [9] for the graph signal \mathbf{x} is defined as a set of filters L_{LP} , L_{HP} , and L_{INV} , where L_{LP} and L_{HP} keep the low-frequency and high-frequency components of \mathbf{x} , respectively. L_{INV} is an inverse filter that obtains an estimate of the input signal $\hat{\mathbf{x}}$ from \mathbf{y}_{LP} and \mathbf{y}_{HP} , which are down-sampled from $\tilde{\mathbf{y}}_{\text{LP}} = L_{\text{LP}} \mathbf{x}$ and $\tilde{\mathbf{y}}_{\text{HP}} = L_{\text{HP}} \mathbf{x}$, respectively. The filters L_{LP} together with L_{HP} are called *analysis filters* and L_{INV} is called a *synthesis filter*. The filter bank is said to satisfy the *perfect reconstruction* property if it is lossless, *i.e.* original graph signals can be exactly reconstructed using a synthesis filter. A good set of analysis filters should have perfect reconstruction property, capable of capturing local (high-frequency) and global (low-frequency) information of graph signals. In the following parts, we focus on implementing analysis filters in GNNs.

3 From One-Pass to Two-Pass: Why and How?

In this section, we state why it is better to switch to the two-pass filtering process from only one-pass. Then, we propose two assistive ideas that are needed to carry out two-pass

learning more considerably, including separate non-linear transformations and adaptive activation.

3.1 Spline-like Filter Banks and Spatial Convolution

Inspired by the classical first-order spline-filters, [10] designs simple two-channel spline-like filters for circulant graphs, which take uniform averages with direct neighbors for the LP filter and uniform differences for the counterpart. This operation can be extended to general graphs [9]:

$$(x_i)_{\text{LP}} = \frac{1}{2} \left[x_i + \sum_{j \in \mathcal{N}_i} w_{ij} x_j \right], \quad (x_i)_{\text{HP}} = \frac{1}{2} \left[x_i - \sum_{j \in \mathcal{N}_i} w_{ij} x_j \right] \quad (4)$$

where w_{ij} is the weight between two nodes. Simple as they are, perfect reconstruction property is proved to be satisfied. The aggregator in the famous GraphSAGE [14] is actually a special case of $(x_i)_{\text{LP}}$, constraining $w_{ij} = A_{ij}/D_{ii}$. In fact, most of the current methods and variants only implement special one-channel (LP) first-order spline filter, incapable of perfect reconstruction. To capture more complete neighborhood information (LP captures similarity with neighborhood while HP captures the difference from the neighborhood), architectures should be equipped with an additional HP channel.

3.2 Spline-like Filters in Matrix Forms

According to [10], LP and HP filters in (4) can be expressed succinctly as follows,

$$L_{\text{LP}}^{\gamma} = Z_{\text{rw}}^{\gamma} = \frac{1}{1 + \gamma} (\gamma I + P_{\text{rw}}), \quad L_{\text{HP}}^{\gamma} = I - Z_{\text{rw}}^{\gamma} = \frac{1}{1 + \gamma} (I - P_{\text{rw}}) \quad (5)$$

where γ can be a learnable or a fixed value. We can see that when $\gamma = 1$, $L_{\text{LP}} = Z_{\text{rw}}$. And since lazy random walk eliminates the bipartite subgraphs in \mathcal{G} , we have $\lambda_i(L_{\text{LP}}) \in (0, 1]$ and $\lambda_i(L_{\text{HP}}) \in [0, 1)$. We have flexibility in (5) to replace P_{rw} by other transition or affinity matrices to form new LP filters, and the HP output can be obtained by subtracting the LP filtered signal from the original signal, similar to the Laplacian pyramid method [26, 9].

Spline-like filters in (4) and (5) are easy to be implemented in most spatial- and spectral-based GNNs. For demonstration, we incorporate these filterbanks to two classic methods, GCN [17] and GraphSAGE [14] in the experiment section.

Necessity of HP Filters Mathematically, LP (aggregation) is a linear projection, which means no matter what features we have learned, it will be projected to a fixed subspace. This means we will lose the expressive power by only using LP filter and this is one major cause of the loss of rank problem in output layer [21]. The missing half is the HP part of the learned signals, as $L_{\text{LP}} + L_{\text{HP}} = I$.

3.3 Separate Nonlinear Feature Extraction Before Filtering

Before filtering, there is often a learnable linear transformation by parameter matrix, which can be interpreted as first to learn a shared linear projection for all nodes and then use the predefined filter to select parts of the projection.

For one-pass filtering, there is only one kind of information that is extracted for filtering (low-pass), while for two-pass filtering, HP and LP filters need to prioritize on the interested information of the layer input in different manners. To make sure the information fed to the two filters are distinctly different and not equivalent after linear transformation, we implement two separate non-linear transformations on the input to excavate the information that each filter needs. This is easily implemented with, *e.g.*,

$$H^1 = f(\hat{A}_{\text{rw}} \cdot f(XW))$$

where f is the activation function. This is equivalent to merging a single layer fully connected network (FCN) [13] and a graph filter in one hidden layer, which could also be expected

to increase the expressive power. Stronger deep networks, *e.g.*, MLP [13], ResNet [15] and DenseNet [16], can also be employed in place of one layer FCN for extraction¹.

3.4 Activation Functions as Graph Filters

In this subsection, we show that (pointwise) activation functions can be analyzed from a graph signal filtering perspective. With this, we show that ReLU is a frequency suppressor and argue for the necessity of activation functions of adaptive behavior for the two passes, since the two passes want the signals (non-linear-)filtered differently before being fed into the aggregator / diversifier.

3.4.1 ReLU as Graph Filter

We abuse $A \in \mathbb{R}^{N \times N}$ to represent a general graph filter. Our question is, if we consider $\text{ReLU}(A \cdot) : \mathbb{R}^N \rightarrow \mathbb{R}^N$ and $\text{AReLU}(A \cdot) : \mathbb{R}^N \rightarrow \mathbb{R}^N$ as two nonlinear graph filters, how will they process an input signal \mathbf{x} . The first problem is how to measure the changes of signal before and after filtering. According to Courant-Fischer theorem [12], we define the singular values for $\text{ReLU}(A \cdot)$ and $\text{AReLU}(A \cdot)$ as follows.

Definition 1. Let $\text{ReLU}(A \cdot)$ and $\text{AReLU}(A \cdot)$ be two operators that map $\mathbb{R}^N \rightarrow \mathbb{R}^N$. Let \mathcal{S} denote a subspace of \mathbb{R}^N . Then, for $i = 1, \dots, N$

$$\begin{aligned}\sigma_i(\text{ReLU}(A \cdot)) &= \min_{\dim(\mathcal{S})=n-i+1} \max_{\mathbf{x} \in \mathcal{S}, \|\mathbf{x}\|_2=1} \|\text{ReLU}(A\mathbf{x})\|_2 \\ \sigma_i(\text{AReLU}(A \cdot)) &= \min_{\dim(\mathcal{S})=n-i+1} \max_{\mathbf{x} \in \mathcal{S}, \|\mathbf{x}\|_2=1} \|\text{AReLU}(A\mathbf{x})\|_2\end{aligned}\quad (6)$$

From the above definition, we can show that

Theorem 1. Given the definition of singular values in (6), we have

$$\sigma_i(\text{ReLU}(A \cdot)) \leq \sigma_i(A), \quad \sigma_i(\text{AReLU}(A \cdot)) \leq \sigma_i^2(A) \quad (7)$$

Proof. See Appendix A. □

The result is consistent with Lemma 5 in [8] based on a different but related definition for singular values of $\text{ReLU}(A \cdot)$ and $\text{AReLU}(A \cdot)$.

ReLU acts like a frequency suppressor and help A to attenuate some components in nonlinear way. And from the proof of Theorem 1, if the inner product (similarity) of a graph signal \mathbf{x} and the neighborhood structure $A_{i,:}$ is negative, \mathbf{x} will be filtered out at node i . In other cases, if a large inner product value appears in the learning process, ReLU is not able to relieve the numerical stability issue. Thus, to make the network more flexible and stable, we propose AdaReLU, which is LeakyReLU with an adaptive truncation threshold as follows

$$\text{AdaReLU}(x_i) = \begin{cases} T, & x_i \geq T \\ \text{LeakyReLU}(x_i), & x_i \leq T \end{cases} \quad (8)$$

where T is a threshold value to clip large values in \mathbf{x} . We can set T to be a constant or an adaptive value, *e.g.*, $\frac{\|\mathbf{x}\|_2}{\sqrt{N}}$, $\frac{\|\mathbf{x}\|_1}{N}$ or $\frac{\|\mathbf{x}\|_2}{\|\mathbf{x}\|_0}$, through which we can eliminate some extreme values in \mathbf{x} adaptively. This provides the possibility for the two-passes to eliminate their noises adaptively in their own fashion.

See Appendix B for the analysis of general nonlinear activation functions.

4 Filter Bank assisted Graph Neural Networks (FB-GNNs)

The two-pass learning framework is provided in figure 1.

¹In empirical tests of this paper, we chose 1 layer for it is lightweight and easier to train.

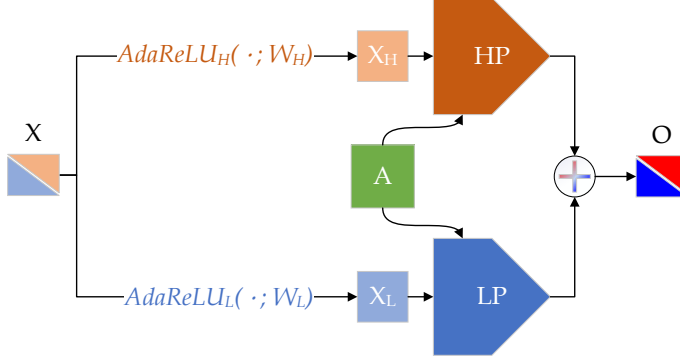


Figure 1: Two-Pass Learning: Information needed for high pass and low pass filters, X_H and X_L , are separately extracted from the input signal X by non-linear transformation powered by the proposed adaptive activation function. After being filtered by HP and LP, both derived upon adjacency matrix A , the filtered signals (HP and LP) are again recombined to form the output O .

4.1 Spectral-based FB-GNNs

We use the two-channel filterbanks defined in 3.2 to define FB-GNNs as follows

$$\mathbf{H}^0 = \mathbf{X}, \mathbf{H}_L^l = L_{LP}f(\mathbf{H}^{l-1}W_L^{l-1}), \mathbf{H}_H^l = L_{HP}f(\mathbf{H}^{l-1}W_H^{l-1}), \quad l = 1, \dots, n \quad (9)$$

where L_{LP} and L_{HP} can be any filterbanks defined as (5), f is activation function, $W_L^{l-1}, W_H^{l-1} \in \mathbb{R}^{F_{l-1} \times F_l}$ are learnable parameter matrices at l -th layer focusing on extracting the smooth and bumpy information from input \mathbf{H}^{l-1} , separately. There are several ways to put \mathbf{H}_L^l and \mathbf{H}_H^l together, e.g.,

$$\mathbf{H}^l = C_l \cdot \mathbf{H}_L^l + (2 - C_l) \cdot \mathbf{H}_H^l, \text{ or } \mathbf{H}^l = [\mathbf{H}_L^l, \mathbf{H}_H^l]W^l \quad (10)$$

where $C_l \in [0, 2]$, $W^l \in \mathbb{R}^{2F_l \times F_l}$ are learnable parameters and parameter matrix. They can learn the relative importance of \mathbf{H}_L^l and \mathbf{H}_H^l and keep a balance between them.

4.2 Spatial-based FB-GNNs

Inspired by (4), the two-channel spatial-based method can be implemented by designing aggregator and diversification operator as follows,

$$\begin{aligned} (\hat{\mathbf{h}}_i^l)_L &= f(W_L^{l-1} \mathbf{h}_i^{l-1}), \quad (\hat{\mathbf{h}}_i^l)_H = f(W_H^{l-1} \mathbf{h}_i^{l-1}), \quad i = 1, \dots, N \\ (\mathbf{h}_i^l)_L &= \frac{1}{1 + \gamma} \sum_{j=1}^N \mathbf{w}_j \left(\frac{1}{\gamma} (\hat{\mathbf{h}}_i^l)_L + (\hat{\mathbf{h}}_j^l)_L \right), \quad (\mathbf{h}_i^l)_H = \frac{1}{1 + \gamma} \sum_{j=1}^N \mathbf{w}_j \left((\hat{\mathbf{h}}_i^l)_H - (\hat{\mathbf{h}}_j^l)_H \right), \quad l = 1, \dots, n \end{aligned} \quad (11)$$

where $W_L^{l-1}, W_H^{l-1} \in \mathbb{R}^{F_l \times F_{l-1}}$ are learnable parameter matrices to extract LP and HP features for two channels, \mathbf{w} is the weight defined in affinity matrices, γ is the predefined or learnable self-loop parameter. The filterbank defined by generalized lazy random walk in (5) can be described as follows

where γ can be a predefined hyperparameter or a learnable parameter.

$$\mathbf{h}_i^l = C_l \cdot (\mathbf{h}_i^l)_L + (2 - C_l) \cdot (\mathbf{h}_i^l)_H, \text{ or } \mathbf{h}_i^l = W^l [(\mathbf{h}_i^l)_L \| (\mathbf{h}_i^l)_H] \quad (12)$$

where $C_l \in [0, 2]$, $W^l \in \mathbb{R}^{F_l \times 2F_{l-1}}$ are learnable parameters and parameter matrix and $\|$ is a concatenation operator. The spatial method is called FB-GraphSAGE.

Computational Cost: Parameters and Runtime The spectral 2-pass learning introduces additionally one GCN operation and one weighted sum (with negligible costs introduced with non-linearity and weighted sum before output); For spatial methods, similarly, the two-pass learning introduces one additional node-wise subtraction and one additional weighted sum for training on each pair of nodes. Thus, the computational cost and the number of parameters are approximately doubled;

For runtime, overlooking the minor overhead of synchronization, the computations introduced with the additional pass are naturally parallelizable with the original pass (for their independently associated parameters) both in the forward and backward passes. Therefore, no significant additional computational time will be incurred on modern GPU architectures.

5 Experiments

In this section, we first validate the effectiveness of the proposed ideas with a detailed ablation test and then validate whether the 2-pass learning leads to better representation learning when patched on popular baselines. The validations are conducted both in the form of node classification and graph classification. The node classification tasks are performed on the datasets Cora, CiteSeer, PubMed and PPI; While the graph classification tasks [32] are conducted on datasets MUTAG [6], PROTEINS [1], PTC [25] and NCI1 [28]. Throughout the whole section, we use 1-layer non-linear transformation, *i.e.* linear transformation followed by non-linear activation, for lightweight training.

5.1 Ablation Tests

The first set of experiments focuses on validating the effectiveness of the individual components proposed in this paper, as well as the effectiveness when they are combined. For this test, we deploy GCN and the patched methods on Cora, as well as GraphSAGE (with mean aggregator) and the patched methods on PPI. Each method on each task is fine-tuned with Bayesian optimization [24] to the same extent². The micro-F1 scores are provided in Table 1 together with their standard deviations obtained from 20 independent runs.

Table 1: Results of Ablation Studies

#channels	non-linear	AdaReLU	GCN @ Cora		GraphSAGE @ PPI	
			F1-mean	F1-std	F1-mean	F1-std
1	N	N	80.5	0.8	59.4	0.8
1	N	Y	82.7	0.5	67.2	0.3
1	Y	N	82.5	0.7	69.5	0.3
1	Y	Y	82.6	0.5	70.5	0.4
2	N	N	82.9	0.6	71.8	0.6
2	N	Y	83.1	0.6	73.5	0.5
2	Y	N	83.0	0.8	73.9	0.4
2	Y	Y	83.6	0.5	75.0	0.7

Color indicators are added for each task, the greener the better performance, the redder the worse. The best performance on each task is marked bold. Each result is featured with the mean micro-F1 scores and their standard deviation, retrieved from 20 runs.

The F1 results show significance of the 3 proposed individual components. We observe that, consistently, when the 3 components are all adopted, the performance boost is the most significant. Therefore, we can say that the proposed components for enabling 2-pass learning can indeed improve graph representation learning.

5.2 Potential for Performance Boost

In this set of experiments, we investigate how much 2-pass learning enhances the performance of existing graph representation learning paradigms. Here, we employ 2 different types

²The search stops after no performance improvement for 64 steps and the search ranges for hyperparameters are the same. More details in the Appendix.

of tasks, node classification and graph classification, with the baseline methods GCN [17] and GraphSAGE [14] against the patched methods FB-GCN and FB-GraphSAGE on node-classification, as well as the baselines GIN-0 and GIN- ϵ [31] against the patched methods FB-GIN-0 and FB-GIN- ϵ . Respecting the pervasive metrics, on node classification, we compare the classification accuracy of methods, with the exception of micro-F1 scores on node classification on PPI.

For the node classification tasks, we use the settings suggested in [33] and [14]. The results of the baselines³ are from [20, 14]. On the node classification tasks, GraphSAGE [14] (with mean, lstm and pool aggregators) and its variant FB-GraphSAGE, conduct inductive learning, as they are trained in nodewise fashion; On the other hand, GCN adopts transductive learning style as it needs the information of the whole graph while training. The hyperparameters are also tuned with Bayesian optimization, to the same extent⁴. The details for hyperparameter search are provided in the Appendix. The results of the node classification tasks are provided in Table 2. From the results, we can see consistent significant performance boost upon the baselines.

Table 2: Results of Node Classification Tasks

Method \ Dataset	Cora		CiteSeer		PubMed		PPI-mean		PPI-pool		PPI-lstm	
	mean	std	mean	std	mean	std	mean	std	mean	std	mean	std
GraphSAGE	74.5%	0.8%	67.2%	1.0%	76.8%	0.6%	59.8	1.2	60.5	0.9	61.2	1.1
<i>FB</i> -GraphSAGE	77.0%	1.0%	71.5%	0.5%	81.1	1.2%	75.0	0.8	75.6	1.0	77.6	1.0
GCN	80.5%	0.8%	68.1%	1.3%	77.8%	0.7%						
<i>FB</i> -GCN	83.6%	0.5%	73.8%	0.6%	79.8%	0.6%						

GCN was not tested on PPI therefore we didn't test it and the patched method on PPI. The best performance on each dataset is marked bold. Each result is featured with the mean scores and its standard deviation, retrieved from 20 independent runs for each test case.

For the graph classification tasks, we compare the patched methods FB-GIN-0 and FB-GIN- ϵ against the baselines GIN-0 and GIN- ϵ , with the same experiment setting as [31]. Hyperparameters are reported in Appendix C. The results (accuracy and standard deviation) are provided in Table 3.

Table 3: Results of Graph Classification Tasks

Method \ Dataset	MUTAG		PROTEIN		PTC		NCI1	
	mean	std	mean	std	mean	std	mean	std
GIN-0	89.4%	5.6%	76.2%	2.8%	64.6%	7.0%	82.7%	1.7%
<i>FB</i> -GIN-0	91.7%	1.2%	80.7%	1.6%	67.4%	6.2%	84.4%	1.5%
GIN- ϵ	89.0%	6.0%	75.9%	3.8%	63.7%	8.2%	82.7%	1.6%
<i>FB</i> -GIN- ϵ	90.4%	3.2%	80.1%	2.2%	66.7%	4.5%	84.3%	0.8%

From the results we can see the patched methods gain significant performance boost compared to the baselines. Also, it is worth noting that the patched methods have less noisy results compared to the baselines, observing from the standard deviation.

6 Conclusion

This paper recognizes the role of high-frequency information in graph representation learning. The proposed HP filter completes the spectrum of graph filters and yield significant performance boost on empirical tests.

³We did not take the results from the original papers for they are not featured with std.

⁴Except for PPI tasks, we used the same hyperparameters reported in GraphSAGE for the baselines as well as the patched methods.

Broader Impact

This paper contributes an fundamental methodology that could enrich the representation learning on graph structures. The method can be easily patched on the existing GNN paradigms with different training strategies. The paper could potentially increase the performance of the existing GNN methods and those to come, and may motivate the research into investigating better graph operations, which will lead to better development of the field.

This work does not present any foreseeable societal consequence.

References

- [1] K. M. Borgwardt, C. S. Ong, S. Schönauer, S. Vishwanathan, A. J. Smola, and H.-P. Kriegel. Protein function prediction via graph kernels. *Bioinformatics*, 21(suppl_1):i47–i56, 2005.
- [2] J. Bruna, W. Zaremba, A. Szlam, and Y. LeCun. Spectral networks and locally connected networks on graphs. *arXiv*, abs/1312.6203, 2014.
- [3] F. Chung and W. Zhao. Pagerank and random walks on graphs. In *Fete of combinatorics and computer science*, pages 43–62. Springer, 2010.
- [4] F. R. Chung and F. C. Graham. *Spectral graph theory*. Number 92. American Mathematical Soc., 1997.
- [5] M. Daković, L. Stanković, and E. Sejdić. Local smoothness of graph signals. *Mathematical Problems in Engineering*, 2019, 2019.
- [6] A. K. Debnath, R. L. Lopez de Compadre, G. Debnath, A. J. Shusterman, and C. Hansch. Structure-activity relationship of mutagenic aromatic and heteroaromatic nitro compounds. correlation with molecular orbital energies and hydrophobicity. *Journal of medicinal chemistry*, 34(2):786–797, 1991.
- [7] M. Defferrard, X. Bresson, and P. Vandergheynst. Convolutional neural networks on graphs with fast localized spectral filtering. *arXiv*, abs/1606.09375, 2016.
- [8] S. Dittmer, J. Emily, and P. Maass. Singular values for relu layers. *IEEE transactions on neural networks and learning systems*, 2019.
- [9] V. N. Ekambaram. *Graph structured data viewed through a fourier lens*. University of California, Berkeley, 2014.
- [10] V. N. Ekambaram, G. Fanti, B. Ayazifar, and K. Ramchandran. Wavelet-regularized graph semi-supervised learning. In *2013 IEEE Global Conference on Signal and Information Processing*, pages 423–426. IEEE, 2013.
- [11] J. Gilmer, S. S. Schoenholz, P. F. Riley, O. Vinyals, and G. E. Dahl. Neural message passing for quantum chemistry. In *Proceedings of the 34th International Conference on Machine Learning-Volume 70*, pages 1263–1272. JMLR. org, 2017.
- [12] G. H. Golub and C. F. Van Loan. *Matrix computations*, volume 3. JHU press, 2012.
- [13] I. Goodfellow, Y. Bengio, and A. Courville. *Deep learning*. MIT press, 2016.
- [14] W. L. Hamilton, R. Ying, and J. Leskovec. Inductive representation learning on large graphs. *arXiv*, abs/1706.02216, 2017.
- [15] K. He, X. Zhang, S. Ren, and J. Sun. Deep residual learning for image recognition. In *Proceedings of the IEEE conference on computer vision and pattern recognition*, pages 770–778, 2016.
- [16] G. Huang, Z. Liu, L. Van Der Maaten, and K. Q. Weinberger. Densely connected convolutional networks. In *Proceedings of the IEEE conference on computer vision and pattern recognition*, pages 4700–4708, 2017.
- [17] T. N. Kipf and M. Welling. Semi-supervised classification with graph convolutional networks. *arXiv*, abs/1609.02907, 2016.
- [18] Y. LeCun, Y. Bengio, and G. Hinton. Deep learning. *nature*, 521(7553):436, 2015.
- [19] Y. LeCun, L. Bottou, Y. Bengio, P. Haffner, et al. Gradient-based learning applied to document recognition. *Proceedings of the IEEE*, 86(11):2278–2324, 1998.
- [20] R. Liao, Z. Zhao, R. Urtasun, and R. S. Zemel. Lanczosnet: Multi-scale deep graph convolutional networks. *arXiv*, abs/1901.01484, 2019.
- [21] S. Luan, M. Zhao, X.-W. Chang, and D. Precup. Break the ceiling: Stronger multi-scale deep graph convolutional networks. *arXiv preprint arXiv:1906.02174*, 2019.
- [22] T. Maehara. Revisiting graph neural networks: All we have is low-pass filters. *arXiv preprint arXiv:1905.09550*, 2019.
- [23] F. Monti, D. Boscaini, J. Masci, E. Rodola, J. Svoboda, and M. M. Bronstein. Geometric deep learning on graphs and manifolds using mixture model cnns. In *Proceedings of the IEEE Conference on Computer Vision and Pattern Recognition*, pages 5115–5124, 2017.

- [24] B. Shahriari, K. Swersky, Z. Wang, R. P. Adams, and N. de Freitas. Taking the human out of the loop: A review of bayesian optimization. *Proceedings of the IEEE*, 104(1):148–175, 2016.
- [25] H. Toivonen, A. Srinivasan, R. D. King, S. Kramer, and C. Helma. Statistical evaluation of the predictive toxicology challenge 2000–2001. *Bioinformatics*, 19(10):1183–1193, 2003.
- [26] P. P. Vaidyanathan. Multirate digital filters, filter banks, polyphase networks, and applications: a tutorial. *Proceedings of the IEEE*, 78(1):56–93, 1990.
- [27] P. Velickovic, G. Cucurull, A. Casanova, A. Romero, P. Lio, and Y. Bengio. Graph attention networks. *arXiv*, abs/1710.10903, 2017.
- [28] N. Wale, I. A. Watson, and G. Karypis. Comparison of descriptor spaces for chemical compound retrieval and classification. *Knowledge and Information Systems*, 14(3):347–375, 2008.
- [29] F. Wu, T. Zhang, A. H. d. Souza Jr, C. Fifty, T. Yu, and K. Q. Weinberger. Simplifying graph convolutional networks. *arXiv preprint arXiv:1902.07153*, 2019.
- [30] Z. Wu, S. Pan, F. Chen, G. Long, C. Zhang, and P. S. Yu. A comprehensive survey on graph neural networks. *arXiv*, abs/1901.00596, 2019.
- [31] K. Xu, W. Hu, J. Leskovec, and S. Jegelka. How powerful are graph neural networks? *arXiv preprint arXiv:1810.00826*, 2018.
- [32] P. Yanardag and S. Vishwanathan. Deep graph kernels. In *Proceedings of the 21th ACM SIGKDD International Conference on Knowledge Discovery and Data Mining*, KDD ’15, page 1365–1374, New York, NY, USA, 2015. Association for Computing Machinery.
- [33] Z. Yang, W. W. Cohen, and R. Salakhutdinov. Revisiting semi-supervised learning with graph embeddings. *arXiv preprint arXiv:1603.08861*, 2016.
- [34] S. Zhang, H. Tong, J. Xu, and R. Maciejewski. Graph convolutional networks: a comprehensive review. *Computational Social Networks*, 6(1):11, 2019.

A Proof of Theorems and Lemmas

Theorem 1. Given the definition of singular values in (6), we have

$$\sigma_i(\text{ReLU}(A \cdot)) \leq \sigma_i(A), \sigma_i(A\text{ReLU}(A \cdot)) \leq \sigma_i^2(A) \quad (13)$$

Proof. For ReLU, we have

$$\text{ReLU}(x) = \begin{cases} x, & x > 0 \\ 0, & x \leq 0 \end{cases} = \delta_x(\mathbb{R}^*) \cdot x \quad (14)$$

Then for $\text{ReLU}(A \cdot)$ and any \mathbf{x} , we have

$$\begin{aligned} \text{ReLU}(Ax) &= \begin{bmatrix} \delta_{\{A_1, \mathbf{x}\}}(\mathbb{R}^*)A_{1,:}\mathbf{x} \\ \delta_{\{A_2, \mathbf{x}\}}(\mathbb{R}^*)A_{2,:}\mathbf{x} \\ \vdots \\ \delta_{\{A_N, \mathbf{x}\}}(\mathbb{R}^*)A_{N,:}\mathbf{x} \end{bmatrix} \\ &= \begin{bmatrix} \delta_{\{A_1, \mathbf{x}\}}(\mathbb{R}^*) & 0 & \cdots & 0 \\ 0 & \delta_{\{A_2, \mathbf{x}\}}(\mathbb{R}^*) & \cdots & 0 \\ \vdots & \vdots & \ddots & \vdots \\ 0 & 0 & \cdots & \delta_{\{A_N, \mathbf{x}\}}(\mathbb{R}^*) \end{bmatrix} Ax \\ &= \Delta_{Ax}(\mathbb{R}^*)Ax \end{aligned} \quad (15)$$

Since $\Delta_{Ax}(\mathbb{R}^*)$ is a diagonal matrix with diagonal element 0 or 1 and thus, $\|\Delta_{Ax}(\mathbb{R}^*)\|_2 \leq 1$. Given the definition (6) and for any \mathbf{x} , we have

$$\|\text{ReLU}(Ax)\|_2 \leq \|\Delta_{Ax}(\mathbb{R}^*)\|_2 \|Ax\|_2 \leq \|Ax\|_2 \quad (16)$$

Suppose $A = U\Sigma V^T$, where $\Sigma = \text{diag}(\sigma_1, \dots, \sigma_r, 0, \dots, 0)$, $V = [\mathbf{v}_1, \mathbf{v}_2, \dots, \mathbf{v}_N]$ and $\mathcal{S}_i = \text{span}(\mathbf{v}_1, \dots, \mathbf{v}_{i-1})^\perp$. Since we know,

$$\sigma_i = \min_{\dim(\mathcal{S})=n-i+1} \max_{\mathbf{x} \in \mathcal{S}, \|\mathbf{x}\|_2=1} \|Ax\|_2 = \max_{\mathbf{x} \in \mathcal{S}_i, \|\mathbf{x}\|_2=1} \|Ax\|_2 \quad (17)$$

Then, for $i = 1, \dots, n$

$$\begin{aligned} \sigma_i(A) &= \max_{\mathbf{x} \in \mathcal{S}_i, \|\mathbf{x}\|_2=1} \|Ax\|_2 \geq \max_{\mathbf{x} \in \mathcal{S}_i, \|\mathbf{x}\|_2=1} \|\text{ReLU}(Ax)\|_2 \\ &\geq \min_{\dim(\mathcal{S})=n-i+1} \max_{\mathbf{x} \in \mathcal{S}, \|\mathbf{x}\|_2=1} \|\text{ReLU}(Ax)\|_2 = \sigma_i(\text{ReLU}(A \cdot)) \end{aligned}$$

Consider the operator $A\text{ReLU}(A \cdot)$ and since A and Δ_{Ax} are symmetric and $\Delta_{Ax}^2 = \Delta_{Ax}$, then for any \mathbf{x}

$$\begin{aligned} \|A\text{ReLU}(Ax)\|_2 &= \|A\Delta_{Ax}(\mathbb{R}^*)Ax\|_2 = \|A\Delta_{Ax}(\mathbb{R}^*)\Delta_{Ax}(\mathbb{R}^*)Ax\|_2 \\ &= \|A^T\Delta_{Ax}(\mathbb{R}^*)^T\Delta_{Ax}(\mathbb{R}^*)Ax\|_2 = \|(\Delta_{Ax}(\mathbb{R}^*)A)^T\Delta_{Ax}(\mathbb{R}^*)Ax\|_2 \end{aligned} \quad (18)$$

Let $B_{Ax} = \Delta_{Ax}(\mathbb{R}^*)A$ and for simplification, we write B_{Ax} as B . We already know $\sigma_i(B) \leq \sigma_i(A)$. Suppose the singular value decomposition of B gives $B = U_B^T \Sigma_B V_B$, then

$$\begin{aligned} \|A\text{ReLU}(Ax)\|_2 &= \|B^T Bx\|_2 = \|V_B^T \Sigma_B U_B U_B^T \Sigma_B V_B x\|_2 \\ &= \|V_B^T \Sigma_B^2 V_B x\|_2 \end{aligned} \quad (19)$$

Then

$$\begin{aligned} \sigma_i(A\text{ReLU}(A \cdot)) &= \min_{\dim(\mathcal{S})=n-i+1} \max_{\mathbf{x} \in \mathcal{S}, \|\mathbf{x}\|_2=1} \|A\text{ReLU}(Ax)\|_2 \\ &= \min_{\dim(\mathcal{S})=n-i+1} \max_{\mathbf{x} \in \mathcal{S}, \|\mathbf{x}\|_2=1} \|V_B^T \Sigma_B^2 V_B x\|_2 \\ &= \sigma_i^2(B) = \sigma_i^2(\text{ReLU}(A \cdot)) \leq \sigma_i^2(A) \end{aligned}$$

Naturally, for the operator $\text{ReLU}(A(\cdots \text{ReLU}(A \cdot) \cdots))$ which composites $\text{ReLU}(A \cdot)$ for n times, we have

$$\sigma_i(\text{ReLU}(A(\cdots \text{ReLU}(A \cdot) \cdots))) \leq \sigma_i^n(A) \quad (20)$$

□

B Proof For Nonlinear Activation Functions

Suppose the activation function f is infinitely differentiable at 0. Consider the operator $f(A \cdot)$ operating on \mathbf{x} , we have

$$\begin{aligned}
f(A\mathbf{x}) &= \begin{bmatrix} f(A_{1,:}\mathbf{x}) \\ f(A_{2,:}\mathbf{x}) \\ \vdots \\ f(A_{N,:}\mathbf{x}) \end{bmatrix} = \begin{bmatrix} \sum_{i=0}^{\infty} f^{(i)}(0)/(i!) \cdot (A_{1,:}\mathbf{x})^i \\ \sum_{i=0}^{\infty} f^{(i)}(0)/(i!) \cdot (A_{2,:}\mathbf{x})^i \\ \vdots \\ \sum_{i=0}^{\infty} f^{(i)}(0)/(i!) \cdot (A_{N,:}\mathbf{x})^i \end{bmatrix} \\
&= \sum_{i=0}^{\infty} f^{(i)}(0)/(i!) \cdot \begin{bmatrix} (A_{1,:}\mathbf{x})^i \\ (A_{2,:}\mathbf{x})^i \\ \vdots \\ (A_{N,:}\mathbf{x})^i \end{bmatrix} \\
&= \sum_{i=0}^{\infty} f^{(i)}(0)/(i!) \cdot \begin{bmatrix} A_{1,:}\mathbf{x} & 0 & \cdots & 0 \\ 0 & A_{2,:}\mathbf{x} & \cdots & 0 \\ \vdots & \vdots & \ddots & \vdots \\ 0 & 0 & \cdots & A_{N,:}\mathbf{x} \end{bmatrix}^{i-1} \begin{bmatrix} A_{1,:}\mathbf{x} \\ A_{2,:}\mathbf{x} \\ \vdots \\ A_{N,:}\mathbf{x} \end{bmatrix} \\
&= f(0)\mathbf{1}_N + \sum_{i=0}^{\infty} f^{(i+1)}(0)/((i+1)!) \cdot \text{diag}([A_{1,:}\mathbf{x}, \dots, A_{N,:}\mathbf{x}])^i A\mathbf{x} \\
&= f(0)\mathbf{1}_N + g(\text{diag}([A_{1,:}\mathbf{x}, \dots, A_{N,:}\mathbf{x}])) A\mathbf{x} \\
&= f(0)\mathbf{1}_N + \text{diag}([g(A_{1,:}\mathbf{x}), \dots, g(A_{N,:}\mathbf{x})]) A\mathbf{x}
\end{aligned}$$

where

$$\begin{aligned}
g(x) &= \sum_{i=0}^{\infty} f^{(i+1)}(0)/((i+1)!)x^i \\
&= \begin{cases} f'(0), & x = 0 \\ (f(x) - f(0))/x, & \text{otherwise} \end{cases}
\end{aligned} \tag{21}$$

It is easy to have

$$\begin{aligned}
&\|f(A\mathbf{x})\|_2 \\
&= \|f(0)\mathbf{1}_N + \text{diag}([g(A_{1,:}\mathbf{x}), \dots, g(A_{N,:}\mathbf{x})]) A\mathbf{x}\|_2 \\
&\leq \|f(0)\mathbf{1}_N\|_2 + \|\text{diag}([g(A_{1,:}\mathbf{x}), \dots, g(A_{N,:}\mathbf{x})])\|_2 \|A\mathbf{x}\|_2 \\
&= \|f(0)\mathbf{1}_N\|_2 + \max_i |g(A_{i,:}\mathbf{x})| \|A\mathbf{x}\|_2
\end{aligned}$$

The last equation holds because the 2-norm of a diagonal matrix is its largest absolute diagonal element. From the definition 1, we have

$$\begin{aligned}
\sigma_i(f(A \cdot)) &\leq f(0) \sqrt{N} + \max_{\|\mathbf{x}\|_2=1} \max_i (|g(A_{i,:}\mathbf{x})| \cdot \|A\mathbf{x}\|_2) \\
&\leq f(0) \sqrt{N} + \left(\max_{\|\mathbf{x}\|_2=1} \max_i |g(A_{i,:}\mathbf{x})| \right) \cdot \left(\max_{\|\mathbf{x}\|_2=1} \|A\mathbf{x}\|_2 \right) \\
&\leq f(0) \sqrt{N} + \left(\max_{\|\mathbf{x}\|_2=1} \max_i |g(A_{i,:}\mathbf{x})| \right) \cdot \sigma_i(A)
\end{aligned} \tag{22}$$

From the above analysis we can see that $f(0) \sqrt{N}$ and $\max_{\|x\|_2=1} \max_i |g(A_{i,:}x)|$ are critical values to bound the filtering effect of the activation function. Since a large family of activation functions are monotonically increasing, we should do truncation to control the upper bound not to be too high.

C Hyperparameters for Experiments

Table 4: FB-GCN Hyperparameters

dataset	lr	decay	width	depth	dropout	acc
Cora	2.4e-3	1.4e-3	1550	1	0.988	83.6
Citeseer	6.4e-3	3.3e-4	100	1	0.566	73.8
Pubmed	7.3e-4	2.8e-4	1100	1	0.858	79.8

Table 5: FB-GraphSAGE Hyperparameters

dataset	lr	decay	dimension	neighbors	dropout	acc
Cora	5.0e-4	6.0e-4	128	30	0.80	77
Citeseer	6.0e-4	6.0e-4	128	35	0.70	71.5
Pubmed	7.0e-3	6.0e-4	128	35	0.70	81.1

Table 6: Graph Classification Hyperparameters

Task	Method	lr	weight decay	gamma	width	batch size	final_output	concat
MUTAG	GIN-0	0.01	0.005		16	32	0	
	FB-FIN-0	0.025878	0.0034029	-0.44504	128	32	0.34121	0
	GIN-eps	0.01	0.005		32	128	0	
	FB-GIN-eps	0.004182	0.029517		64	32	0.59501	1
PROTEINS	GIN-0	0.01	0.005		16	32	0	
	FB-FIN-0	0.007066	0.017799	-0.01868	8	32	0.68011	0
	GIN-eps	0.01	0.005		16	128	0.5	
	FB-GIN-eps	0.002616	0.046504		64	32	0.42657	1
PTC	GIN-0	0.01	0.005		32	32	0.5	
	FB-FIN-0	0.006683	0.0062857	-0.13761	64	128	0.16032	1
	GIN-eps	0.01	0.005		16	32	0.5	
	FB-GIN-eps	0.000502	0.034352		16	32	0.99719	0
NCI1	GIN-0	0.01	0.005		32	32	0	
	FB-FIN-0	0.000406	0.16032	0.03647	128	128	0.088672	1
	GIN-eps	0.01	0.005		32	32	0	
	FB-GIN-eps	0.000796	0.031205		128	128	0.017387	0